Received: 26 November 2021 | Revised: 8 April 2022 | Accepted: 8 April 2022

DOI: 10.1002/suco.202100832

ARTICLE

fib CEB-FIP WILEY

Electrical resistivity measurements to determine the steel fiber content of concrete

Simon Cleven | **Michael Raupach** | **Thomas Matschei**

Institute of Building Materials Research, RWTH Aachen University, Aachen, Germany

Correspondence
Simon Cleven, Institute of Building Materials Research, RWTH Aachen University, Schinkelstr. 3, 52062 Aachen, Germany.
Email: cleven@ibac.rwth-aachen.de

Abstract

Although steel fiber reinforced concrete is becoming increasingly popular in the construction industry, its application is currently limited to certain areas. One reason is the lack of an economical non-destructive testing method to determine the content, distribution, and orientation of steel fibers in fresh and hardened concrete. However, these parameters are decisive for the assessment of the static performance of a building component. In this article a new test method is proposed, which is based on the electrical conductivity of concrete. Using a two-electrode experimental set-up, measurements of the electrical conductivity were done on hardened concrete cubes with defined fiber content and a correlation between electrical conductivity and fiber content could be identified. Within the scope of extensive test series, the fiber content and the age of specimens were varied, and several identical series were produced and observed to ensure statistically verified results. At this stage of research the test method based on electrical conductivity measurement provides reliable results on the fiber content of preconditioned concrete cubes. Based on the results a new model was developed to quantify the fiber content of the examined cubes. This model is based on the estimation of the relative conductivity, the so-called increase of conductivity. Undesired influences caused by aging, respectively hydration in the young concrete age were eliminated, by relating the conductivity of fiber reinforced concrete to an unreinforced concrete. Further investigations with focus on the influence of concrete composition and other specimen sizes are going to be conducted as next steps for the development of an in situ test setup for the diagnosis of concrete structures.

KEYWORDS

electrical conductivity, fiber content, non-destructive test method, steel fiber reinforced concrete

Discussion on this paper must be submitted within two months of the print publication. The discussion will then be published in print, along with the authors' closure, if any, approximately nine months after the print publication.

1 | INTRODUCTION

Steel fiber reinforced concrete (SFRC) is a commonly used material for civil construction. It consists of plain concrete (PC) and macroscopic steel fibers, which are mostly produced out of wires (see, e.g., Refs. 1–6). SFRC combines positive features from both of its components and compensates their disadvantages. PC as an unreinforced material is nearly freely shapeable and can resist high compressive loads, but nearly no tensile stresses, whereas drawn steel wires are characterized as reinforcements with an extremely high tensile strength. The combination of the materials leads to an improvement of tensile strength, ductility, and impact strength (see, e.g., Refs. 7–11). As alternative material for conventional steel reinforced concrete in some cases, constructions can be planned and realized with SFRC without the time-consuming process of reinforcing. Because of limitations of the tensile strength in ultimate limit stage in comparison to steel reinforced concrete, the main application of SFRC can be found in constructions with lower static requirements, which is why SFRC is often used for industrial floorings, residential construction. Also, underground construction in the form of precast tunnel segments, so called tubbings, which have the highest static requirements in building condition, can be an interesting application for SFRC (see, e.g., Refs. 12–14).

The mechanical parameters of SFRC are strongly affected by the content of fibers in the concrete, their distribution and orientation. All three parameters show a considerable influence on the load bearing capacity after initial cracking of the concrete (see e.g., Ref. 15–19). In general, the flexural strength of SFRC lies in between the ones of PC and conventional steel reinforced concrete, but with high amounts of steel fibers a ductile and strengthening behavior after first crack building in concrete can be observed. Lower dosages of fibers lead to a strain softening behavior, but nevertheless a significant increase of its residual strength in comparison to PC and a uniform and fine crack distribution (see, e.g., Refs. 7–11).

One challenge in the use of SFRC is the uneven und often unknown distribution and orientation of the fibers in concrete elements. While the global fiber content can be controlled by a precise dosing process, the local parameters can deviate from the global ones. Based on this problem, relatively large deviations of up to 20% of test results for mechanical properties can occur. Therefore, the safety factors for the static calculations must be high to ensure a secure way of construction (see, e.g., Refs. 20–23). Also, the orientation of fibers has a big effect on the strength of the compound material. The maximum load transmission between two crack edges can be reached by fibers that are oriented parallel to the applied stress. In this position the angle between the fiber and the crack is 90°. A decrease of this angle leads to a significant decrease of the transmittable tensile strength (see, e.g., Refs. 24–26). For these reasons, the knowledge of the local fiber content and their orientation is of great importance for test specimens and for construction elements. Various test setups have been developed and applied in scientific studies. So far, no accurate and easy to apply setup was found, which can be used for in situ monitoring or at the construction site.

The highest detailed and specific results on fiber content, distribution and orientation in concrete specimens can be obtained by computer tomographic analysis (see, e.g., Refs. 27–33). With high effort and expensive equipment, a 3-dimensional visualization of the specimen is possible, where the fibers and concrete can be distinguished by their different densities. The biggest problems of this test method, however, are the excessive costs for the equipment and the relatively small specimens that can be analyzed.

An easier setup can be used to generate 2-dimensional sectional images of SFRC, the so-called photo-optical method. Based on a large number of sectional images an acceptable evaluation of the fiber amount and orientation in different areas of concrete elements is possible (see, e.g., Refs. 34 and 35). Even so the equipment for this method is much cheaper it is a very time-consuming work because many sectional images out of different sections of the specimens and of course in different orientations are needed to get a sufficient overview of a structural element. Other methods based on inductivity (see, e.g., Refs. 36–46) or permittivity (see, e.g., Refs. 47–54) are also used in scientific research but cannot be realized yet in the process of construction of huge elements or even buildings. An example for a test setup using permittivity measurements of SFRC is given in Ref. 53, where an open-ended coaxial probe is applied to the surface of concrete slabs. Although the laboratory results show that the determination of the fiber volume fraction is possible, using this method, a high effort of equipment and time, especially for applying complex models with different simplifying assumptions, is necessary.

For that reason, first results of an experimental program using electrical resistivity measurements on SFRC to set up a model for fiber content, distribution, and orientation of distinct types of specimens are presented in this paper. Electrical resistivity measurements are currently used for the monitoring of the corrosion behavior of steel rebars in concrete elements using multiring-electrodes (see, e.g., Refs. 55–59). By extending this idea, the objective of this study is to develop a test setup that can be adapted on nearly all types of concrete elements

and can be used for in situ measurements on SFRC buildings (see, e.g., Refs. 60–63). In a first step, separately cast cubic specimens with a defined concrete composition are investigated to get a basic approach and correlation between the electrical resistivity of SFRC and its fiber content. Further investigations are ongoing to extend the setup to cylindrical specimens, like drilling cores, and with help of finite element modeling to structural elements or whole concrete structures. Even if this further development will be much more complicated and time consuming, the presented study shall be the first step of the development.

2 | EXPERIMENTAL PROGRAM

2.1 | Materials

To investigate the influence of fiber content, distribution, and orientation in concrete specimens on the electrical resistivity, respectively, electrical conductivity, of the SFRC, specimens of one type of concrete mixture with varying fiber content have been produced. To eliminate possible influences of supplementary cementitious materials, ordinary Portland cement was used as binder. The water/cement-ratio was set to 0.45. For the aggregates, a quarzitic material with a fine grain size distribution of C16 according to DIN 1045-2[64] was used. The maximum grain size of 16 mm was chosen to ensure a nearly free distribution of the fibers without a considerable influence of the biggest grains. The cement content was set to 470 kg/m^3 to attain a high workability and low porosity of the concrete mixture without the use of superplasticizer. The mix design of the resulting concrete is presented in Table 1.

The production of the concrete was done in the following way. First the cement and the aggregates were homogenized in a compulsory mixer with a nominal volume of 160 L. After 30 s the water was added, and the concrete was mixed for at least 2 min. Then the PC was visually inspected, and the walls of the mixer were scratched from adhering components and an additional mixing phase of 1 min was performed. Afterward the target consistency of the PC was examined via flow table test in accordance with EN 12350-5[65] and the air content and fresh concrete density were determined in accordance with EN 12350-6[66] respectively EN 12350-7[67]. Each concrete production was performed with a material volume of 70 L. Following the fresh concrete testing, samples of 4 L each were extracted of the mixer and placed in a bucket mixer. Also, a defined fiber content of 10–120 kg/m^3, appropriate to 0.1%–1.5% by volume, was added in the mixer and mixed for about 1 min before the concrete was filled into cubical steel formworks with dimensions of 150 mm^3. Before the casting of the formworks, the SFRC was visually inspected to ensure that no negative effects of the fiber addition, like agglomerations of fibers or an insufficiently high porosity, took place. Although the maximum fiber content of 120 kg/m^3 was very high, no defects in the concrete structure could be identified. Additionally, one PC specimen without fibers was produced. The used fibers were hooked steel fibers with a length of 60 mm, a diameter of 1 mm and a tensile strength of about 1500 N/mm^2. This procedure was performed six times, so there are six identical series of specimens with different fiber contents from 0 to 120 kg/m^3, what gives in total 72 specimens.

TABLE 1 Concrete mix design

Parameter	Unit	Content
CEM I 52.5 R	kg/m^3	470.0
Water		211.5
Aggregates		
Milisil W3		218.3
0.1–0.5 mm		326.9
0.5–1.0 mm		238.4
1.0–2.0 mm		210.0
2.0–4.0 mm		186.8
4.0–8.0 mm		234.9
8.0–16.0 mm		193.8
Total		1609.1
Water/cement-ratio	—	0.45

2.2 | Test setup

All specimens were stored in the formworks, covered with foil, for 1 day. After demolding, the upper surfaces of the specimen were ground down to ensure a flat surface for a good electric connection. Then the specimens were stored in separate storage boxes under water at a temperature of 20°C till testing.

Because of the small dimensions of the specimens in relation to the fiber length an electric connection over the entire sample surface areas was chosen to reduce effects of single fibers or grains near the surfaces. To compare different geometries of the specimen, the specific resistance respectively conductivity values can be calculated by using absolute values and a geometrical factor k. The specific values are necessary to compare different specimens and represent independent material properties. In the case of a full connection of two parallel

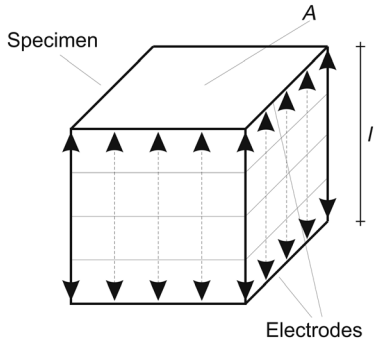

FIGURE 1 Shape of the electric field of two parallel electrodes

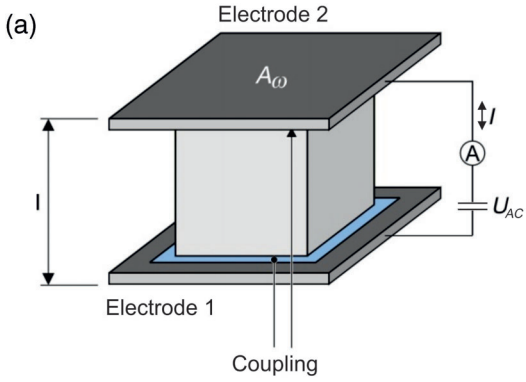

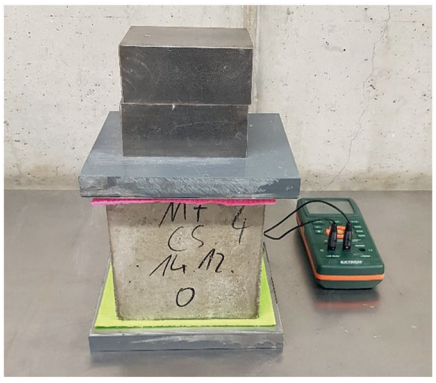

FIGURE 2 Scheme of the test setup (a) and photo of the test setup (b) for conductivity measurements

surfaces of a specimen the shape of the electric fields can be described as shown in Figure 1. The factor k for this configuration of electrodes can be calculated by the percolated area A and the distance of the electrodes l by following Equation (1):

$$k = A/l \tag{1}$$

where, k is the geometry factor depending on dimensions of specimens in m; A is the effective contact area in m^2; l is the electrode gap in m.

TABLE 2 Parameters of the resistivity analysers

Parameter	LCR meter	Potentiostat
Type designation	Extech Instruments LCR200	Gamry Instruments 1010E
AC amplitude	600 mV rms	17.8 μV to 2.33 V
Frequency	100 Hz, 120 Hz, 1 kHz, 10 kHz, 100 kHz	10 μHz to 2 MHz
Measuring range of impedance	0.000 Ω to 200.0 MΩ	
Accuracy	±0.5%	±0.5%

The resulting test setup consists of two electrodes made of stainless steel with an edge length of 200 mm to inhibit corrosive effects on the surfaces, which are connected to a resistivity analyzer with identical cables. Since the connection to the concrete surface solely by the steel electrode was not possible in a reproducible way, a wetted sponge cloth was used to allow a connection over the entire surface. The moisture of the sponge clothes was constantly checked and adjusted with fresh water, tempered to 20°C. The full test setup can be seen as schema in Figure 2a, and a picture of the setup is presented in Figure 2b.

Every specimen was evaluated in all three directions to receive results of the global fiber content and values for different orientations of the specimens. Before the measurement was performed, a single specimen was taken out of its storage box and the surface water was removed by using paper towels. Then the specimen was placed on the first electrode and the second one was placed on top. To obtain a constant und reproducible contact pressure a defined reference weight was placed on top of the test setup.

As resistivity analyzers two different devices were used, depending on the investigated parameters. The first on was a so called LCR meter, type Extech Instruments LCR 200, and the second one was a potentiostat, type Gamry Instruments 1010E. The parameters of both devices can be found in Table 2.

By use of the LCR meter an alternating current (AC) with a voltage amplitude of about 600 mV rms was induced at a fixed frequency. For the measurements in this study all possible frequencies were used. The LCR meter then reports the electrical resistance as resulting parameter. After the measurement of all frequencies in one direction of the cube, it was turned around until all three possible directions were analyzed.

By use of a digital potentiostat different amplitudes of AC as well as different frequencies were assessed. In one continuous test series the amplitude of the AC was

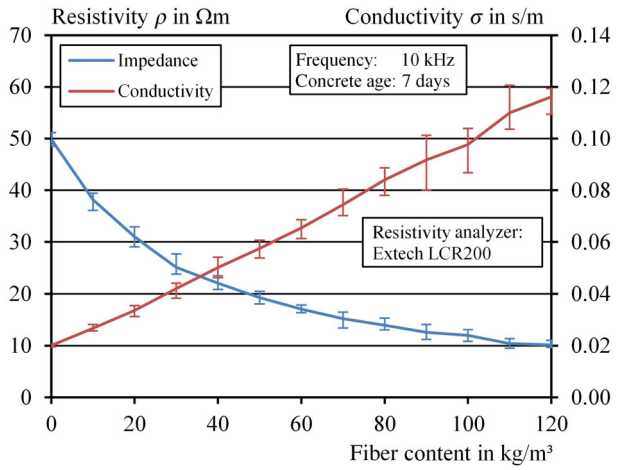

FIGURE 3 Correlation between electrical resistivity, respectively, conductivity and fiber content, resistivity analyzer: Extech Instruments LCR200

changed in the range of 10–200 mV while the frequencies varied between 1 Hz and 100 kHz on one SFRC specimen (see Section 3.3). Due to the continuous monitoring only one direction of the specimen was evaluated. Another series of tests was performed at a constant amplitude and only varying frequency over a period of about 17 h to identify effects of drying of the coupling and the specimens on both PC and SFRC (see Section 3.2).

3 | RESULTS AND DISCUSSION

3.1 | Correlation between electrical resistivity and fiber content

All results confirm a considerable influence of the fiber content onto the measured electrical resistivity respectively conductivity of the investigated SFRC specimens. The results presented in Figure 3 include all six series of each 13 specimens, investigated by use of the device Extech Instruments LCR200. The electrical resistivity combines both the conductivity of the steel fibers and of the concrete. A deviation in results could be seen which is based on the inhomogeneity and anisotropy of the material. The maximum coefficient of variation of 9.65% was found for a fiber content of 90 kg/m^3. A relation between fiber content and deviation could not be identified. Usually, conductivity is a homogenous parameter for isotropic materials, but in case of SFRC the calculation of a global value of the specific material's resistance as mean value of all three cube directions was necessary. The global conductivity was calculated analogously. The presented values were measured at a frequency of 10 kHz for a concrete age of 7 days.

It is obvious that the addition of fibers to the concrete led to a higher conductivity or lower electrical resistivity. Especially low fiber dosages showed a high impact on the measured electrical resistivity, whereas at higher fiber dosages the differences were less clear. An addition of 30 kg/m^3 of fiber to the unreinforced concrete resulted in a bisection of the electrical resistivity from about 50 to 25 Ωm. When another 30 kg/m^3 of fibers were added the loss of electrical resistivity was only about 30%, so there is no linear correlation between fiber content and electrical resistivity. In contrast it could be seen that the conductivity nearly correlates to the fiber content in a linear way.

3.2 | Influence of frequency and measuring time

To evaluate the influence of the frequency and the measuring period in detail the test setup was changed for two additional measurements. For this test series the potentiostat (Gamry Instruments 1010E) was used to get results of different frequencies over a prolonged period of time. The specimen without fibers was analyzed at a concrete age of 14 days, in only one direction because the potentiostat was able to log results continuously over a period of about 17 h whereat the frequency was varied from 1 Hz to 100 kHz. The influence of the measuring time on the electrical resistivity is presented in Figure 4.

Because of the higher concrete age of 14 days, the electrical resistivity in general was higher than for the same specimen at a concrete age of 7 days (cf. Figure 3). This phenomenon will be investigated in detail in Section 3.4. It can be determined that in the first 30 min there was an increase in electrical resistivity, followed by

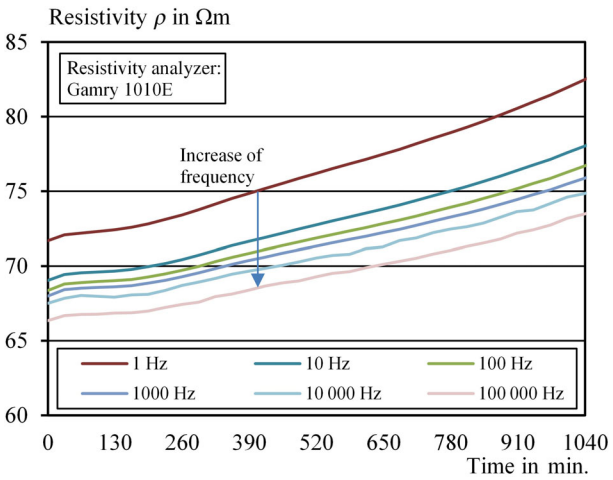

FIGURE 4 Effect of varying measuring time on the electrical resistivity of PC, resistivity analyzer: Gamry Instruments 1010E

a small plateau and another nearly linear increase until the end of the observations. This behavior occurred independently from frequency of AC, whereat an increase of the electrical resistivity could be observed with increasing frequency. The time-depending effects can be explained by the drying process of the sponge cloths and the concrete and the resulting loss of saturation of the pore structure, which is the conductive part of both the concrete and the sponge cloths. The dehydration process starts at the surface of the concrete, but a small reservoir of water can possibly be found in the sponge cloth that serves for the connection of the electrodes.

During the first minutes the loss of moisture of those couplings is high because of the open pore system of the surface dry concrete specimen. After a first water exchange process the moisture of the coupling and the concrete will be balanced and the water exchange will nearly stop. But after a time both materials will start to interact with the surrounding air, which has a lower moisture content and so a dehydration process of the whole measuring system will start. For the measuring process the conclusion can be drawn that the time of contact of specimen and coupling should be minimized, and the sponge cloths must be kept in a nearly constant condition of moisture.

In Figure 5 a predictable loss of electrical resistivity with increasing frequency could be observed, which was nearly independent from the moisture of the coupling, what is clearly visible through the parallelism of the single curves for different measuring times. In general, the fact that an increase of humidity leads to a decrease of the electrical resistivity, which is described above as well as in earlier studies of the autors (see Ref. 68), also can be identified in this figure. The single curves can be divided by dashed lines into three parts, based on different sectors of frequency. In the first sector, between frequencies of 1 Hz to about 50 Hz, a disproportional decrease of the electrical resistivity was visible. An explanation of this behavior can be found in polarization effects which can appear on both electrodes at low frequencies and are the reason to use AC instead of direct current (DC) in this study. At higher frequencies in sector two there was a linear decrease of the electrical resistivity, followed by another disproportional descending above a frequency of 10 kHz in sector three, that can be explained by inductive effects in cables or connections of the measuring system. For the following measurements based on these results it was decided to investigate the electrical resistivity in the range of 100 Hz to 100 kHz to avoid polarization effects that possibly modify the concrete surfaces or couplings of the system.

As can be seen in Figure 6, which shows the complete set of data of the investigations of measuring time and frequency, both parameters show a huge effect on the electrical resistivity, while there is no influence of the parameters among each other.

The same results could be identified on a SFRC specimen with 80 kg/m^3 of fibers (Figure 7). This specimen was tested at a concrete age of 14 days in one horizontal direction so that the fibers were supposed to show a huge effect because it can be assumed that most of the fibers will be oriented in horizontal direction when the specimens are produced in layers and compacted on a vibration table. As can be seen the influence of the frequency on the electrical resistivity was significantly higher for SFRC than for unreinforced concrete for frequencies

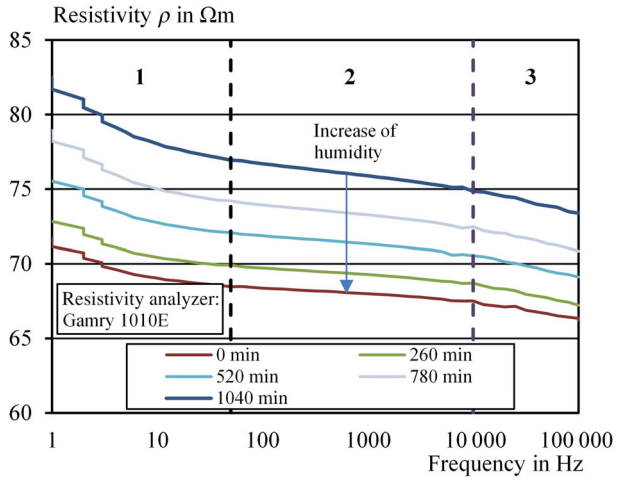

FIGURE 5 Effect of varying frequency on the electrical resistivity of concrete, resistivity analyzer: Gamry Instruments 1010E

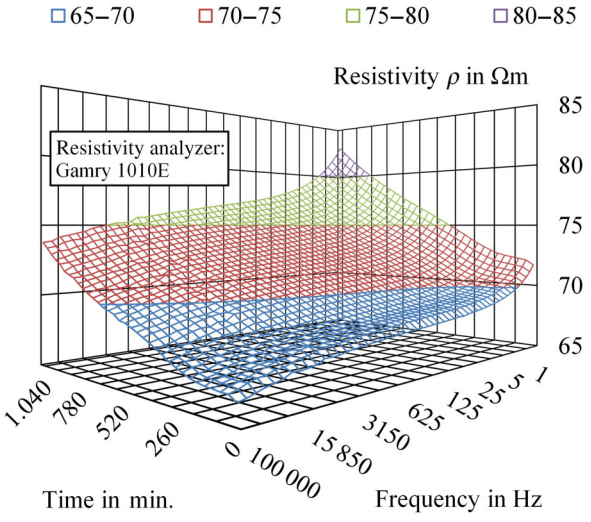

FIGURE 6 Effect of varying frequency and measuring time on the electrical resistivity of PC, resistivity analyzer: Gamry Instruments 1010E

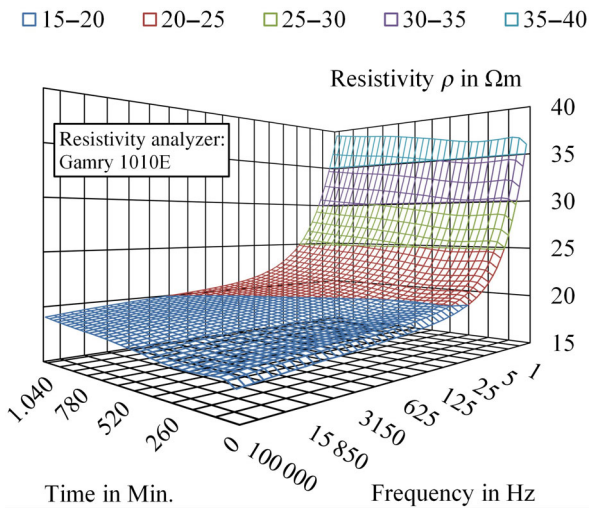

FIGURE 7 Effect of varying frequency and measuring time on the electrical resistivity of SFRC with a fiber dosage of 80 kg/m^3, resistivity analyzer: Gamry Instruments 1010E

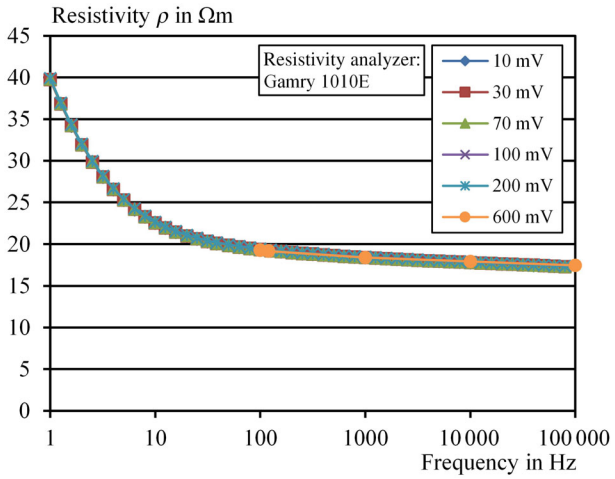

FIGURE 8 Effect of varying amplitudes on the electrical resistivity of SFRC, resistivity analyzer: Gamry Instruments 1010E

below 10 Hz. This is probably based on the polarization effects on every connection point of fiber and concrete which takes part in the electrical connection. Because of the high effect of the frequency the measuring time or dehydration status of the specimen becomes subordinated. A comparison of both figures leads to the conclusion, that a higher frequency is better for the differentiation of the fiber content because at low frequencies a fiber content of 80 kg/m^3 resulted in a doubling of the electrical resistivity whereas at high frequencies it led to a nearly four times higher electrical resistivity so the selectivity of the results will be higher.

3.3 | Influence of amplitude

Another parameter to be investigated was the amplitude of the AC. With help of the potentiostat (Gamry Instruments 1010E), different amplitudes in the range of 10–200 mV could be realized in combination with frequencies in the same range than in Section 3.2. The investigation was done to see if any effects, like corrosion or polarization, occur if the amplitude is set too high. To see beneficial effects over a big spread of electrical resistivities, the SFRC specimen containing 80 kg/m^3 of fibers from Section 3.2 was also used in this investigation. This specimen was also evaluated with the LCR meter with a fixed amplitude of 600 mV to see if the LCR meter gives comparable results to the potentiostat. The results in Figure 8 showed no significant effects of the amplitude on the measured electrical resistivity while the influence of the frequency was clearly visible like described in Section 3.2. For the measurements with the potentiostat, frequencies between 1 Hz and 100 kHz were investigated and for the LCR meter only the five frequencies 100 Hz, 120 Hz, 1 kHz, 10 kHz, and 100 kHz were possible. This means that the highest impact of the frequencies on the electrical resistivity was not visible in the results produced with the LCR meter. Because nearly no differences in the measured resistivity for different amplitudes was visible, it can be concluded that in the tested range of amplitudes no damage based on the AC were induced to the concrete. Therefore, the highest amplitude can be used for the further investigations, what will result in the best resolution of the results, because higher voltages will be induced and so the resistivity of the concrete can be calculated with a higher accuracy. This shows that the LCR meter is an appropriate measurement system with the given amplitude of 600 mV.

3.4 | Influence of specimen age

The last investigated parameter in this research was the age of the specimen and so the hydration progress and the resulting pore structure. This effect was analyzed over a period of 56 days, on specimens with fiber contents from 0 to 120 kg/m^3 with the Extech Instruments LCR200 at all five possible frequencies. Like described in Section 3.1, a significant loss of the electrical resistivity was visible with increasing fiber content. This can also be seen in Figure 9 for a frequency of 10 kHz. Also, the hydration changed the electrical resistivity of the PC, respectively of SFRC. With increasing specimen age and therefore increasing hydration process and building of pore structure, an increase of the electrical resistivity is accompanied. The effect from an age of 7–28 days

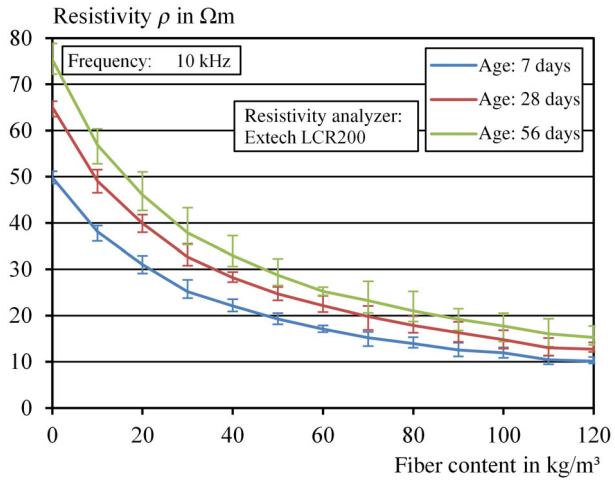

FIGURE 9 Effect of specimen age/storage duration on the electrical resistivity, resistivity analyzer: Extech Instruments LCR200

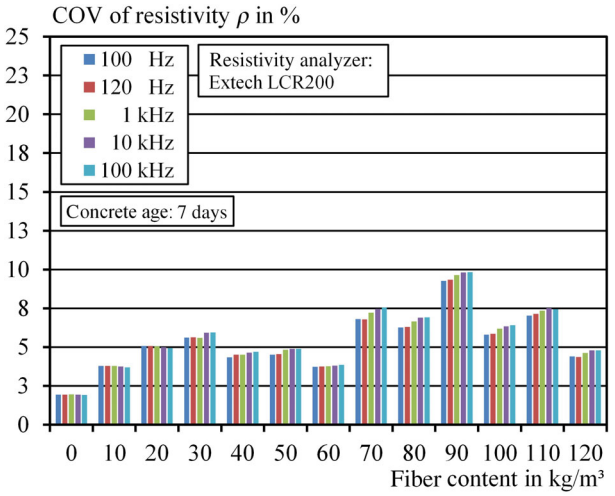

FIGURE 10 COV of the electrical resistivity in measurements at specimen age of 7 days, resistivity analyzer: Extech Instruments LCR200

thereby was bigger than the increase from 28 to 56 days. Because of the used binder, OPC, it is obvious that the greatest part of the hydration will be completed at the age of 28 days, so that most of water will be bound to the cement clinker and the pore structure will be almost finalized. After 28 days the changes in the pore structure will be smaller than in the first days, so the resulting increase in electrical resistivity is also smaller.

The changes of the microstructure based on the hydration process showed a higher effect on concrete with lower fiber dosages, what means that effects on connectivity between fibers and concrete did not take place. With increasing concrete age, the influence of fibers in the concrete on the measured electrical resistivity increased what would be a good tendency for the analysis of structural buildings in case of maintenance and repair. But it should be noted that the age of the concrete must be considered to predict the fiber content of an analyzed concrete based on its electrical resistivity.

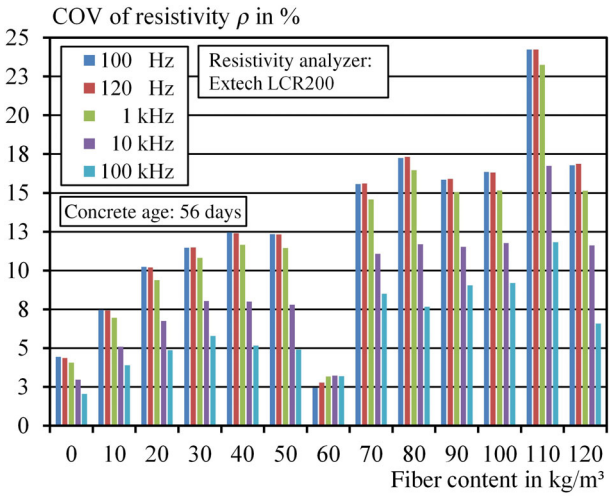

FIGURE 11 COV of the electrical resistivity in measurements at specimen age of 56 days, resistivity analyzer: Extech Instruments LCR200

3.5 | Statistical verification

At the end of investigations the variance of the electrical resistivity of different concrete specimens within the same composition and identical curing conditions was proved by a statistical analysis of all six series of identical concretes with identical curing conditions. A graphical presentation of the coefficients of variation of the electrical resistivities of the specimens with an age of 7 days can be seen in Figure 10. It is evident that the PC without fibers only showed a small spread in the electrical resistivity while the fiber reinforced specimens had slightly bigger COV's. No correlation between fiber content and spread was identified. Therefore, the addition of fibers generally led to an increased COV with respect to the measurement of the electrical resistivity. The main reason seems to be the random distribution and orientation of fibers in the specimen. Also, no significance between the frequency and the spread could be seen in the results of the 7 days old concrete.

In contrast to those results the variance of measurements of the electrical resistivity for the older specimens with an age of 56 days was significantly higher (Figure 11). Even the PC shows a higher COV, for the SFRC specimens, except for a fiber content of 60 kg/m^3, a much higher spread of the electrical resistivity occurred. In this specimen age an effect of the frequency was also

clearly visible. For the frequencies below 10 kHz it seems that with an increasing fiber content the COV of the electrical resistivity likewise increased. With a fiber content of 80 kg/m^3, it seems to be a limit with a COV of about 18% and a further increase of fibers did not lead to a higher spread if the results of a fiber content of 110 kg/m^3 were assessed as outliers.

The positive aspect of these results is that for higher frequencies the spread is significantly smaller and only slightly above the results of the very young concrete. So, the effects of hydration of the concrete within this testing conditions showed the lowest significance. For the development of a model that predicts the fiber content based on measurements of the electrical resistivity, high frequencies should be used to reach statistically valuable results.

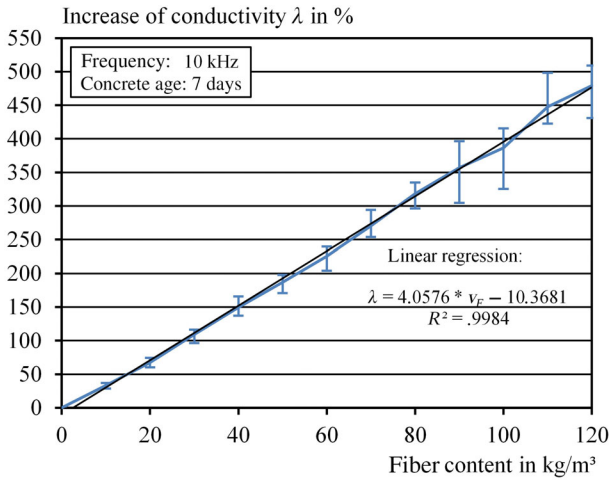

FIGURE 12 Correlation between fiber content and increase of conductivity

4 | DEVELOPMENT OF A PREDICTION METHOD

4.1 | Basic approach

Because of the influence of the specimen age (Section 3.4), the electrical resistivity itself as a direct parameter for the prediction of the fiber content of concrete is not suitable. The conductivity of the concrete is too much influenced by the hydration process and by the humidity of the concrete. Therefore, a parameter must be found that compensates for such effects. Based on physical fundamentals, equivalent circuits were analyzed but because of the inhomogeneity and anisotropy, simple models like parallel connection or series connection were not applicable. For this reason, the increase of conductivity of SFRC relative to the PC λ was calculated for each fiber content by the following Equation (2):

$$\lambda = \sigma_{SFRC}/\sigma_{PC} \quad (2)$$

where, λ is the increase of conductivity in %; σ_{SFRC} is the conductivity of SFRC in s/m; σ_{PC} is the conductivity of PC in s/m.

For developing a prediction method, only the measurements are used, that were performed with use of the Extech Instruments LCR200. The correlation between fiber content and increase of conductivity is presented in Figure 12. A nearly linear correlation between fiber content and increase of conductivity could be observed, where the spread increased with increasing fiber content. This means a relative failure of the correlation of about ±10% could be identified while the mean values showed a coefficient of determination of 0.9984. For the adaption of the test setup as in situ test method for concrete

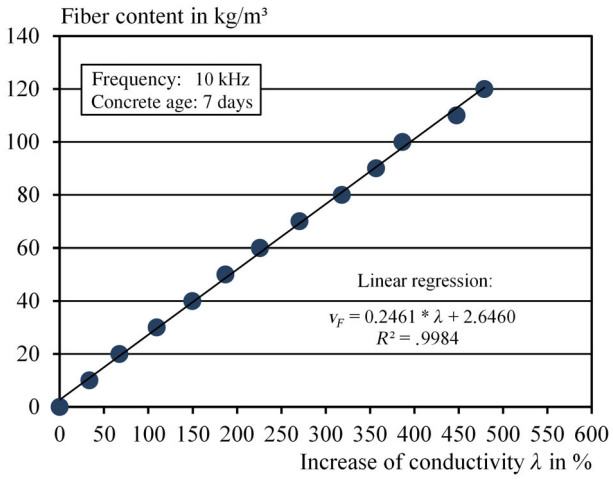

FIGURE 13 Prediction method of fiber content based on increase of conductivity

structures the determination of the conductivity of the PC will be difficult. Investigations of very small volumes of SFRC are going to be performed to check if it is possible to estimate the conductivity of PC without steel fibers if the volume of the specimen or the percolated volume is small enough.

For the prediction of the fiber content the axes of the diagram have been swapped in Figure 13 so the fiber content c_F becomes the result of the calculated increase of conductivity λ. With this diagram and the equation the fiber content of a specimen can be predicted based on the measured electrical resistivity by the following Equation (3):

$$c_F = 0.25 \times \lambda + 2.65 \quad (3)$$

where, c_F is the fiber content in kg/m^3; λ is the increase of conductivity in %.

As can be seen in Equation (3) a higher fiber content goes along with a high increase of conductivity and a linear correlation can be used to display this behavior. One inaccuracy in the function can be found in the axial intercept that deviates from the origin of the coordinate system. Based on theoretical considerations a fiber content of 0 kg/m^3 that represents the PC must lead to an increase of conductivity of 0% but as a result of a limited data base the empirical analysis led to the best agreement of the function and the data with this inaccuracy.

4.2 | Extension to different concrete ages

In the last step the prediction method has been validated with all gained raw data. For this purpose, all single values of the six test series in the three different concrete ages were compared with the basic model from Section 4.1. Also, the mean values of the six series were included in Figure 14. It is evident that the parameter λ gave the possibility to approximate the fiber content of the concrete almost independent to the concrete age from 7 to 56 days. The mean values for all ages showed a good agreement with the regression, while the single values partially differed from it.

With increasing fiber content, the scatter between the model and the single values also increased, what can be interpreted as a relative scatter in material parameters. An absolute error was not visible because for low fiber dosages neither the single values itself showed nearly any deviation nor a difference from the model curve. For the possibility of an approximation of the fiber content via the electrical conductivity this tendency means that an adequate number of specimens must be taken and tested to gain sufficient raw data. Otherwise, large safety factors must be considered to not overestimate the fiber content. With a series of six specimens for example it is possible to estimate the fiber content with an accuracy of ±8%. For fiber contents in the practical range of above 20 kg/m^3 an accuracy of ±3% could be observed. In contrast to the mean values by use of the single values the largest discrepancies in the estimated fiber content to the real one were ±17%.

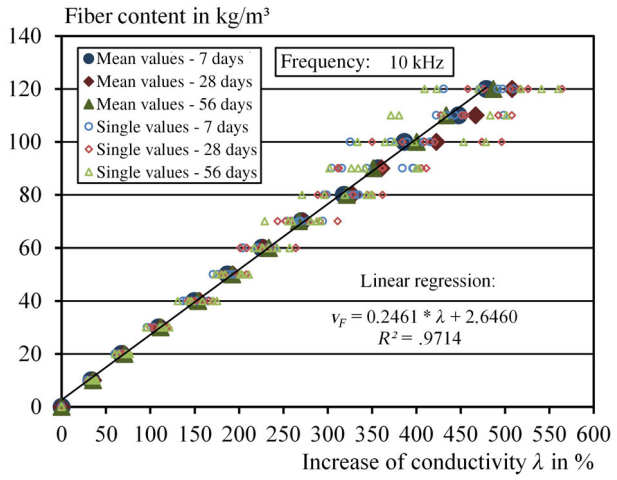

FIGURE 14 Extension of the prediction method to different concrete ages

Looking onto the mean values for the higher concrete ages it can be noticed that the model seemed to be imperfect, since the mean results for high fiber contents from over 100 kg/m^3 did not show a linear trend but the curve bottomed out. With a higher amount of data and even older specimens the model could be optimized to reach a more sufficient estimation. The second problem was the divergence of the model curve from the point of origin. This point represented the PC and so the increase of conductivity using fibers was definitively 0%. For low fiber contents because of this shift of the curve an additional inaccuracy was intrinsic so that a sufficient estimation of contents of about 10 kg/m^3 was not possible. On the other hand, it is questionable if such low fiber contents are used in practice and a need to determine the parameters of the SFRC in detail exists.

5 | CONCLUSIONS

The fiber content is an important parameter which has an immense effect on the mechanical performance of SFRC. Because of the lack of determination methods for the fiber content in hardened concrete, relatively high safety factors must be used in static analysis. Based on the electrical conductivity, a new method was presented to estimate the fiber content of a known concrete mixture with ordinary steel fibers.

To set up this model investigations on concrete specimens with fiber contents from 0 to 120 kg/m^3 were performed and a statistical evaluation was done by the comparison of six series of specimens. The results show an influence of different parameters on the electrical conductivity respectively resistivity. While the amplitude of AC nearly has no effect on the electrical resistivity of SFRC, the frequency must be taken into consideration. Low frequencies especially for SFRC result in a significantly higher electrical resistivity based on polarization effects than frequencies above about 10 kHz, where a nearly constant electrical resistivity can be measured. For PC, the effect of frequency is much smaller, so this parameter could be a good research topic for further studies. The measuring period, synonymous to the dehydration of the

specimens, which were stored under water, shows only a small effect, when it is smaller than a few hours and the biggest effect can be seen on PC. On the contrary an increase of the age of specimen from 7 to 56 days leads to a significant increase of the electrical resistivity because of the change of its pore structure. However, the biggest effect on conductivity results in the addition of fibers which lead to an additional conductive part in the material and therefore increase the conductivity.

By the calculation of the increase of conductivity λ the effects of the aging could be compensated and a linear correlation between fiber content and λ was identified. Based on this correlative model it was validated which accuracy of estimation for the fiber content is possible by measuring the electrical conductivity. It was observed that an amount of six specimens leads to an efficient estimation of the fiber content with deviations of about $\pm$6%, which could help to minimize safety factors for static analysis.

In comparison to different research directions, like the use of microwave analysis of SFRC (see, e.g., Refs. 53,54) the presented method is still limited to concrete specimens and not yet ready for in situ analysis of concrete structures. Nevertheless, the very fast measuring process, the low modeling effort and the observed independence of the results from the concrete hydration, are advantageous compared with permittivity measurements, where a constant behavior is expected only for fully hydrated concrete.

However, it shall be observed in further investigations if the identified model of this study can be optimized by an increased data base and if the effect of different concrete mixtures can be as easily compensated as the different concrete ages. Also, a method shall be identified that allows an estimation of the conductivity of the PC so the test method can be used on concretes in practice when no PC is available. Additionally, in further test series of the authors, the test setup has been modified for tests of cylindrical specimens like drilling cores that can be extracted out of existing structures (see Refs. 69,70). With help of a finite element modeling of the electrical current flow an extension of the test setup is supposable that can be applied directly on structural elements, since it has already been shown for drilling cores. By adopting the finite element model to more difficult geometries, in a first step to precast elements, the possibility of in situ testing of structures shall be analyzed and possible limitations of the test setup shall be identified and removed. One major challenge concerning further development of the presented technique is the need to consider the saturation state, respectively the moisture content, of the concrete to be tested, which varies according to age and geometry of the investigated concrete structures. To address this challenge, preconditioning tests on laboratory concrete samples may be used to derive calibration curves, which enable a subsequent correction of the moisture effect.

DATA AVAILABILITY STATEMENT

The data that support the findings of this study are available from the corresponding author upon reasonable request.

ORCID

Simon Cleven https://orcid.org/0000-0002-2876-1341

REFERENCES

1. Ferdosian I, Camões A. Mechanical performance and post-cracking behavior of self-compacting steel-fiber reinforced eco-efficient ultra-high performance concrete. Cem Concr Compos. 2021;121:104050. https://doi.org/10.1016/j.cemconcomp.2021.104050
2. Lehner P, Konečný P, Ponikiewski T. Comparison of material properties of SCC concrete with steel fibres related to ingress of chlorides. Crystals. 2020;10:220. https://doi.org/10.3390/cryst10030220
3. Ding X, Zhao M, Zhou S, Fu Y, Li C. Statistical analysis and preliminary study on the mix proportion design of self-compacting steel fiber reinforced concrete. Materials. 2019;12(4):637. https://doi.org/10.3390/ma12040637
4. Kachouh N, El-Hassan H, El-Maaddawy T. Effect of steel fibers on the performance of concrete made with recycled concrete aggregates and dune sand. Construct Build Mater. 2019;213:348–59. https://doi.org/10.1016/j.conbuildmat.2019.04.087
5. Shan L, Zhang L. Experimental study on mechanical properties of steel and polypropylene fiber-reinforced concrete. Appl Mech Mater. 2014;2014:1355–61. https://doi.org/10.4028/www.scientific.net/AMM.584-586.1355
6. Di Prisco M, Plizzari G, Vandewalle L. Fibre reinforced concrete: new design perspectives. Mater Struct. 2009;42(9):1261–81. https://doi.org/10.1617/s11527-009-9529-4
7. Luo T, Zhang C, Sun C, Zheng X, Ji Y, Yuan X. Experimental investigation on the freeze–thaw resistance of steel fibers reinforced rubber concrete. Materials. 2020;13:1260. https://doi.org/10.3390/ma13051260
8. Hedjazi S, Castillo D. Effect of fibre types on the electrical properties of fibre reinforced concrete. Mater Express. 2020;10:733–9. https://doi.org/10.1166/mex.2020.1679
9. Kobaka J, Katzer J, Ponikiewski T. A combined electromagnetic induction and radar-based test for quality control of steel fibre reinforced concrete. Materials. 2019;12:3507. https://doi.org/10.3390/ma12213507
10. Zhang P, Li Q, Chen Y, Shi Y, Ling Y. Durability of steel fiber-reinforced concrete containing SiO2 nano-particles. Materials. 2019;12:2184. https://doi.org/10.3390/ma12132184
11. Song PS, Hwang S. Mechanical properties of high-strength steel fiber-reinforced concrete. Construct Build Mater. 2014;18:669–73. https://doi.org/10.1016/j.conbuildmat.2004.04.027
12. Facconi L, Minelli F, Ceresa P, Plizzari G. Steel fibers for replacing minimum reinforcement in beams under torsion.

Mater Struct. 2021;54:34. https://doi.org/10.1617/s11527-021-01615-y
13. Li X, Xue W, Fu C, Yao Z, Liu X. Mechanical properties of high-performance steel-fibre-reinforced concrete and its application in underground mine engineering. Materials. 2019;12:2470. https://doi.org/10.3390/ma12152470
14. Brandt AM. Fibre reinforced cement-based (FRC) composites after over 40 years of development in building and civil engineering. Compos Struct. 2008;86:3–9. https://doi.org/10.1016/j.compstruct.2008.03.006
15. Martinelli P, Colombo M, Pujadas P, De la Fuente A, Cavalaro S, Di Prisco M. Characterization tests for predicting the mechanical performance of SFRC floors: identification of fibre distribution and orientation effects. Mater Struct. 2021;54:1–13. https://doi.org/10.1617/s11527-020-01593-7
16. Martinelli P, Colombo M, De la Fuente A, Cavalaro S, Pujadas P, di Prisco M. Characterization tests for predicting the mechanical performance of SFRC floors: design considerations. Mater Struct. 2021;54:1–16. https://doi.org/10.1617/s11527-020-01598-2
17. Li FY, Li LY, Dang Y, Wu PF. Study of the effect of fibre orientation on artificially directed steel fibre-reinforced concrete. Adv Mater Sci Eng. 2018;2018:1–11. https://doi.org/10.1155/2018/8657083
18. Barnett SJ, Lataste J, Parry T, Millard SG, Soutsos MN. Assessment of fibre orientation in ultra high performance fibre reinforced concrete and its effect on flexural strength. Mater Struct. 2010;43:1009–23. https://doi.org/10.1617/s11527-009-9562-3
19. Gettu R, Gardner DR, Saldívar H, Barragán BE. Study of the distribution and orientation of fibers in SFRC specimens. Mater Struct. 2005;38:31–7. https://doi.org/10.1617/14021
20. Tarawneh A, Almasabha G, Alawadi R, Tarawneh M. Innovative and reliable model for shear strength of steel fibers reinforced concrete beams. Structure. 2021;32:1015–25. https://doi.org/10.1016/j.istruc.2021.03.081
21. Cugat V, Cavalaro SHP, Bairán JM, de la Fuente A. Safety format for the flexural design of tunnel fibre reinforced concrete precast segmental linings. Tunn Undergr Space Technol. 2020;103:103500. https://doi.org/10.1016/j.tust.2020.103500
22. Herrmann H, Boris R, Goidyk O, Braunbrück A. Variation of bending strength of fiber reinforced concrete beams due to fiber distribution and orientation and analysis of microstructure. IOP Conf Ser: Mater Sci Eng. 2019;660(1):012059. https://doi.org/10.1088/1757-899X/660/1/012059
23. Molins C, Aguado A, Saludes S. Double punch test to control the energy dissipation in tension of FRC (Barcelona test). Mater Struct. 2009;42:415–25. https://doi.org/10.1617/s11527-008-9391-9
24. Cao YYY, Yu QL. Effect of inclination angle on hooked end steel fiber pullout behavior in ultra-high performance concrete. Compos Struct. 2018;201:151–60. https://doi.org/10.1016/j.compstruct.2018.06.029
25. Zhou B, Uchida Y. Influence of flowability, casting time and formwork geometry on fiber orientation and mechanical properties of UHPFRC. Cem Concr Res. 2017;1:164–77. https://doi.org/10.1016/j.cemconres.2017.02.017
26. Timmers G, van Mier JGM, Nooru-Mohamed BB. An experimental study of shear fracture and aggregate interlocks in cementbased composites. Heron. 1991;36.
27. Park T, Her S, Jee H, Yoon S, Cho B, Hwang S, et al. Evaluation of orientation and distribution of steel fibers in high-performance concrete column determined via micro-computed tomography. Construct Build Mater. 2021;270:121473. https://doi.org/10.1016/j.conbuildmat.2020.121473
28. Rajeshwari BR, Sivakumar MVN, Praneeth PH. Visualization and quantification of aggregate and fiber in self-compacting concrete using computed tomography for wedge splitting test. Archives of civil and mechanical. Engineering. 2020;20(4):1–16. https://doi.org/10.1007/s43452-020-00140-z
29. Balázs GL, Czoboly O, Lublóy É, Kapitány K, Barsi Á. Observation of steel fibres in concrete with computed tomography. Construct Build Mater. 2017;140:534–41. https://doi.org/10.1016/j.conbuildmat.2017.02.114
30. Ponikiewski T, Katzer J. X-ray computed tomography of fibre reinforced self-compacting concrete as a tool of assessing its flexural behaviour. Mater Struct. 2016;49(6):2131–40. https://doi.org/10.1617/s11527-015-0638-y
31. Suuronen J-P, Kallonen A, Eik M, Puttonen J, Serimaa R, Herrmann H. Analysis of short fibres orientation in steel fibre-reinforced concrete (SFRC) by X-ray tomography. J Mater Sci. 2013;48(3):1358–67. https://doi.org/10.1007/s10853-012-6882-4
32. Nezhentseva A, Sørensen EV, Andersen LV, Schuler F. Distribution and Orientation of Steel Fibres in UHPFRC. Department of Civil Engineering, Aalborg University. DCE Technical Reports No. 151; 2013.
33. Schnell J, Ackermann FP, Rösch R, Sych T. Statistical Analysis of Fibre Distribution in Ultra High Performance Concrete Using Computer Tomography. Kassel: Schriftenreihe Baustoffe und Massivbau; 2008.
34. Lee S, Oh J, Cho J. Fiber orientation factor on rectangular cross-section in concrete members. Int J Eng Technol. 2015;7(6):470–3. https://doi.org/10.7763/IJET.2015.V7.839
35. Zak G, Park CB, Benhabib B. Estimation of three-dimensional fibre-orientation distribution in short-fibre composites by a two-section method. J Compos Mater. 2000;35(4):316–339. https://doi.org/10.1106/65LQ-1UK7-WJ9H-K2FH
36. Li L, Xia J, Chin C, Jones S. Fibre distribution characterization of ultra-high performance fibre-reinforced concrete (uhpfrc) plates using magnetic probes. Materials. 2020;13(22):1–20. https://doi.org/10.3390/ma13225064
37. Lei T, Ottoboni R, Faifer M, Toscani S, Ferrara L. A cost-effective method to assess the fiber content and orientation in steel fiber reinforced concrete. Paper presented at the I2MTC 2019–2019 IEEE International Instrumentation and Measurement Technology Conference; 2019. https://doi.org/10.1109/I2MTC.2019.8827015.
38. Hobst L, Bílek P. Nondestructive identification of material properties of fibre concrete: a stationary magnetic field. AIP Conf Proc. 2016;1738:380010. https://doi.org/10.1063/1.4952171
39. Juan-García P, Torrents JM, López-Carreño RD, Cavalaro SHP. Influence of fiber properties on the inductive method for the steel-fiber-reinforced concrete characterization. IEEE Trans Instrum Meas. 2016;65(8):1937–44. https://doi.org/10.1109/TIM.2016.2549678
40. Mattarneh A-H. Electromagnetic quality control of steel fiber concrete. Construct Build Mater. 2014;73:350–6. https://doi.org/10.1016/j.conbuildmat.2014.09.101

41. Wichmann H-J, Budelmann H, Holst A. Non-destructive measurement of steel fiber dosage and orientation in concrete. In: Büyüköztürk O, Tasdemir MA, Günes O, Akkaya Y, editors. Nondestructive Testing of Materials and Structures, Proceedings of NDTMS-2011, Istanbul. Berlin: Springer; 2011. p. 239–45. https://doi.org/10.1007/978-94-007-0723-8_35
42. Torrents JM, Blanco A, Pujadas P, Aguado A, Juan-García P, Sánchez-Moragues MÁ. Inductive method for assessing the amount and orientation of steel fibers in concrete. Mater Struct. 2012;45(10):1577–92. https://doi.org/10.1617/s11527-012-9858-6
43. Ferrara L, Faifer M, Toscani S. A magnetic method for non destructive monitoring of fiber dispersion and orientation in steel fiber reinforced cementitious composites – part 1: method calibration. Mater Struct. 2012;45:575–89. https://doi.org/10.1617/s11527-011-9793-y
44. Faifer M. Nondestructive testing of steel-fiber-reinforced concrete using a magnetic approach. IEEE Trans Instrum Meas. 2011;2011(60):1709–17. https://doi.org/10.1109/TIM.2010.2090059
45. Faifer M, Ottoboni R, Toscani S. A compensated magnetic probe for steel fiber reinforced concrete monitoring. Proc IEEE Sens. 2010;698–703. https://doi.org/10.1109/ICSENS.2010.5690066
46. Faifer M, Ottoboni R, Toscani S, Ferrara L. Steel fiber reinforced concrete characterization based on a magnetic probe. Paper presented at the 2010 IEEE International Instrumentation and Measurement Technology Conference, I2MTC 2010; 2010. https://doi.org/10.1109/IMTC.2010.5488179.
47. Akgol O, Unal E, Bağmancı M, Karaaslan M, Sevim UK, Öztürk M, et al. A nondestructive method for determining fiber content and fiber ratio in concretes using a metamaterial sensor based on a V-shaped resonator. J Electron Mater. 2019;48(4):2469–81. https://doi.org/10.1007/s11664-019-06937-w
48. Mehdipour I, Horst M, Zoughi R, Khayat KH. Use of near – field microwave reflectometry to evaluate steel fiber distribution in cement – based mortars. J Mater Civil Eng. 2017;29:04017029. https://doi.org/10.1061/(ASCE)MT.1943-5533.0001850
49. Jamil M, Hassan MK, Mattarneh A-HMA, Zain MFM. Concrete dielectric properties investigation using microwave non-destructive techniques. Mater Struct. 2013;46:77–87. https://doi.org/10.1617/s11527-012-9886-2
50. Karlovšek J, Wagner N, Scheuermann A. Frequency-dependant dielectric parameters of steel fiber reinforced concrete. Paper presented at the 2012 14th International Conference on Ground Penetrating Radar, GPR 2012, pp. 510–516; 2012. https://doi.org/10.1109/icgpr.2012.6254918.
51. Roqueta G, Jofre L, Romeu J, Blanch S. Microwave time-domain reflection imaging of steel fiber distribution on reinforced concrete. IEEE Trans Instrum Meas. 2011;60(12):3913–22. https://doi.org/10.1109/TIM.2011.2138330
52. Van Damme S, Franchois A, Pauw DP, Taerwe L. Comparison of two coaxial probes for measuring the steel fiber content in fiber reinforced concrete slabs. 9th International Conference on Electromagnetics in Advanced Applications ICEAA '05; 11th European Electromagnetic Structures Conference EESC '05; September 12–16, 2005; Torino, Italy.
53. Van Damme S, Franchois A, Zutter, De D, Taerwe L. Nondestructive determination of the steel fiber content in concrete slabs with an open-ended coaxial probe. IEEE Trans Geosci Rem Sens. 2004;42:2511–21. https://doi.org/10.1109/TGRS.2004.837332
54. Franchois A, Taerwe L, Van Damme S. A microwave probe for the non-destructive determination of the steel fiber content in concrete slabs. 6th RILEM Symposium on Fibre-Reinforced Concretes (FRC) – BEFIB 2004, 20–22 September 2004, Varenna, Italy.
55. Reichling K, Raupach M, Klitzsch N. Determination of the distribution of electrical resistivity in reinforced concrete structures using electrical resistivity tomography. Mater Corros. 2015;66:763–71. https://doi.org/10.1002/maco.201407763
56. Reichling, K. Bestimmung und Bewertung Des Elektrischen Widerstands von Beton Mit Geophysikalischen Verfahren; Technische Hochschule, Fachbereich 3: Aachen, Dissertation, Germany, 2014.
57. Raupach M, Gulikers J, Reichling K. Condition survey with embedded sensors regarding reinforcement corrosion. Mater Corros. 2013;64:141–6. https://doi.org/10.1002/maco.201206629
58. Reichling K, Raupach M. Measurement and visualisation of the actual concrete resistivity in consideration of conductive layers and reinforcement bars. Concrete Repair, Rehabilitation and retrofitting III-Proceedings of the 3rd International Conference on Concrete Repair, Rehabilitation and Retrofitting. Abingdon, UK: Taylor & Francis Group; 2012. p. 707–14.
59. Raupach M, Dauberschmidt C, Wolff L. Monitoring the moisture distribution in concrete structures. Concrete Repair, Rehabilitation and Retrofitting-Proceedings of the International Conference on Concrete Repair, Rehabilitation and Retrofitting. Boca Raton, FL: CRC Press; 2006. p. 166–7.
60. Ruan T, Poursaee A. Fiber-distribution assessment in steel fiber-reinforced UHPC using conventional imaging, X-ray CT scan, and concrete electrical conductivity. J Mater Civ Eng. 2019;31(8):04019133. https://doi.org/10.1061/(ASCE)MT.1943-5533.0002733
61. Molodtsov MV, Molodtsova VE. Electrical resistivity of steel fiber reinforced concrete. IOP Conf Ser: Mater Sci Eng. 2018;451(1):012079. https://doi.org/10.1088/1757-899X/451/1/012079
62. Uygunoğlu T, Topçu İB, Şimşek B. Influence of steel-fiber type and content on electrical resistivity of old-concrete. Comput Concr. 2018;21(1):1–9. https://doi.org/10.12989/cac.2018.21.1.001
63. Ozyurt N, Woo LY, Mason TO, Shah SP. Monitoring fiber dispersion in fiber-reinforced cementitious materials: comparison of AC-impedance spectroscopy and image analysis. ACI Mater J. 2006;103:340–7.
64. Concrete, Reinforced and Prestressed Concrete Structures—Part 2: Concrete - Specification, Properties, Production and Conformity—Application Rules for DIN EN 206-1; DIN 1045-2: 2008-08. Berlin, Germany: Beuth Publishing DIN; 2008. https://doi.org/10.31030/1453177
65. Testing Fresh Concrete—Part 5: Flow Table Test; German Version EN 12350-5:2019; DIN EN 12350-5:2019-09. Berlin, Germany: Beuth Publishing DIN; 2019. https://doi.org/10.31030/3045714
66. Testing Fresh Concrete—Part 6: Density; German Version EN 12350-6:2019; DIN EN 12350-6:2019-09. Berlin, Germany: Beuth Publishing DIN; 2019. https://doi.org/10.31030/3045731
67. Testing Fresh Concrete—Part 7: Air Content—Pressure Methods; German Version EN 12350-7:2019; DIN EN 12350-7: 2019-09. Berlin, Germany: Beuth Publishing DIN; 2019. https://doi.org/10.31030/3045732

68. Cleven S, Raupach M, Matschei T. Electrical resistivity of steel fibre-reinforced concrete—influencing parameters. Materials. 2021;14:3408. https://doi.org/10.3390/ma14123408
69. Cleven S, Raupach M, Matschei T. A new method to determine the steel fibre content of existing structures—test setup and numerical simulation. Appl Sci. 2022;12:561. https://doi.org/10.3390/app12020561
70. Cleven S, Raupach M, Matschei T. A new method to determine the steel fibre content of existing structures—evaluation and validation. Appl Sci. 2022;12:454. https://doi.org/10.3390/app12010454

AUTHOR BIOGRAPHIES

Simon Cleven
Institute of Building Materials Research
RWTH Aachen University
Schinkelstr. 3
52062 Aachen, Germany.
cleven@ibac.rwth-aachen.de

Univ.-Prof. Dr.-Ing. Michael Raupach
Institute of Building Materials Research
RWTH Aachen University
Schinkelstr. 3
52062 Aachen, Germany.
raupach@ibac.rwth-aachen.de

Univ.-Prof. Dr.-Ing. Thomas Matschei
Institute of Building Materials Research
RWTH Aachen University
Schinkelstr. 3
52062 Aachen, Germany.
matschei@ibac.rwth-aachen.de

How to cite this article: Cleven S, Raupach M, Matschei T. Electrical resistivity measurements to determine the steel fiber content of concrete. Structural Concrete. 2022. https://doi.org/10.1002/suco.202100832